



Measurement of CP -Violation Parameter $\sin 2\phi_1$ with 152 Million $B\bar{B}$ Pairs

K. Abe,⁹ K. Abe,⁴⁴ N. Abe,⁴⁷ R. Abe,³⁰ T. Abe,⁹ I. Adachi,⁹ Byoung Sup Ahn,¹⁶ H. Aihara,⁴⁶ M. Akatsu,²³ M. Asai,¹⁰ Y. Asano,⁵¹ T. Aso,⁵⁰ V. Aulchenko,² T. Aushev,¹³ S. Bahinipati,⁵ A. M. Bakich,⁴¹ Y. Ban,³⁴ E. Banas,²⁸ S. Banerjee,⁴² A. Bay,¹⁹ I. Bedny,² P. K. Behera,⁵² I. Bizjak,¹⁴ A. Bondar,² A. Bozek,²⁸ M. Bračko,^{21, 14} J. Brodzicka,²⁸ T. E. Browder,⁸ M.-C. Chang,²⁷ P. Chang,²⁷ Y. Chao,²⁷ K.-F. Chen,²⁷ B. G. Cheon,⁴⁰ R. Chistov,¹³ S.-K. Choi,⁷ Y. Choi,⁴⁰ Y. K. Choi,⁴⁰ M. Danilov,¹³ M. Dash,⁵³ E. A. Dodson,⁸ L. Y. Dong,¹¹ R. Dowd,²² J. Dragic,²² A. Drutskoy,¹³ S. Eidelman,² V. Eiges,¹³ Y. Enari,²³ D. Epifanov,² C. W. Everton,²² F. Fang,⁸ H. Fujii,⁹ C. Fukunaga,⁴⁸ N. Gabyshev,⁹ A. Garmash,^{2, 9} T. Gershon,⁹ G. Gokhroo,⁴² B. Golob,^{20, 14} A. Gordon,²² M. Grosse Perdekamp,³⁶ H. Guler,⁸ R. Guo,²⁵ J. Haba,⁹ C. Hagner,⁵³ F. Handa,⁴⁵ K. Hara,³² T. Hara,³² Y. Harada,³⁰ N. C. Hastings,⁹ K. Hasuko,³⁶ H. Hayashii,²⁴ M. Hazumi,⁹ E. M. Heenan,²² I. Higuchi,⁴⁵ T. Higuchi,⁹ L. Hinz,¹⁹ T. Hojo,³² T. Hokuue,²³ Y. Hoshi,⁴⁴ K. Hoshina,⁴⁹ W.-S. Hou,²⁷ Y. B. Hsiung,^{27, *} H.-C. Huang,²⁷ T. Igaki,²³ Y. Igarashi,⁹ T. Iijima,²³ K. Inami,²³ A. Ishikawa,²³ H. Ishino,⁴⁷ R. Itoh,⁹ M. Iwamoto,³ H. Iwasaki,⁹ M. Iwasaki,⁴⁶ Y. Iwasaki,⁹ H. K. Jang,³⁹ R. Kagan,¹³ H. Kakuno,⁴⁷ J. Kaneko,⁴⁷ J. H. Kang,⁵⁵ J. S. Kang,¹⁶ P. Kapusta,²⁸ M. Kataoka,²⁴ S. U. Kataoka,²⁴ N. Katayama,⁹ H. Kawai,³ H. Kawai,⁴⁶ Y. Kawakami,²³ N. Kawamura,¹ T. Kawasaki,³⁰ N. Kent,⁸ A. Kibayashi,⁴⁷ H. Kichimi,⁹ D. W. Kim,⁴⁰ Heejong Kim,⁵⁵ H. J. Kim,⁵⁵ H. O. Kim,⁴⁰ Hyunwoo Kim,¹⁶ J. H. Kim,⁴⁰ S. K. Kim,³⁹ T. H. Kim,⁵⁵ K. Kinoshita,⁵ S. Kobayashi,³⁷ P. Koppenburg,⁹ K. Korotushenko,³⁵ S. Korpar,^{21, 14} P. Križan,^{20, 14} P. Krokovny,² R. Kulasiri,⁵ S. Kumar,³³ E. Kurihara,³ A. Kusaka,⁴⁶ A. Kuzmin,² Y.-J. Kwon,⁵⁵ J. S. Lange,^{6, 36} G. Leder,¹² S. H. Lee,³⁹ T. Lesiak,²⁸ J. Li,³⁸ A. Limosani,²² S.-W. Lin,²⁷ D. Liventsev,¹³ R.-S. Lu,²⁷ J. MacNaughton,¹² G. Majumder,⁴² F. Mandl,¹² D. Marlow,³⁵ T. Matsubara,⁴⁶ T. Matsuishi,²³ H. Matsumoto,³⁰ S. Matsumoto,⁴ T. Matsumoto,⁴⁸ A. Matyja,²⁸ Y. Mikami,⁴⁵ W. Mitaroff,¹² K. Miyabayashi,²⁴ Y. Miyabayashi,²³ H. Miyake,³² H. Miyata,³⁰ L. C. Moffitt,²² D. Mohapatra,⁵³ G. R. Moloney,²² G. F. Moorhead,²² S. Mori,⁵¹ T. Mori,⁴⁷ J. Mueller,^{9, †} A. Murakami,³⁷ T. Nagamine,⁴⁵ Y. Nagasaka,¹⁰ T. Nakadaira,⁴⁶ E. Nakano,³¹ M. Nakao,⁹ H. Nakazawa,⁹ J. W. Nam,⁴⁰ S. Narita,⁴⁵ Z. Natkaniec,²⁸ K. Neichi,⁴⁴ S. Nishida,⁹ O. Nitoh,⁴⁹ S. Noguchi,²⁴ T. Nozaki,⁹ A. Ogawa,³⁶ S. Ogawa,⁴³ F. Ohno,⁴⁷ T. Ohshima,²³ T. Okabe,²³ S. Okuno,¹⁵ S. L. Olsen,⁸ Y. Onuki,³⁰ W. Ostrowicz,²⁸ H. Ozaki,⁹ P. Pakhlov,¹³ H. Palka,²⁸ C. W. Park,¹⁶ H. Park,¹⁸ K. S. Park,⁴⁰ N. Parslow,⁴¹ L. S. Peak,⁴¹ M. Pernicka,¹² J.-P. Perroud,¹⁹ M. Peters,⁸ L. E. Piilonen,⁵³ F. J. Ronga,¹⁹ N. Root,² M. Rozanska,²⁸ H. Sagawa,⁹ S. Saitoh,⁹ Y. Sakai,⁹ H. Sakamoto,¹⁷ H. Sakaue,³¹ T. R. Sarangi,⁵² M. Satapathy,⁵² A. Satpathy,^{9, 5} O. Schneider,¹⁹ S. Schrenk,⁵ J. Schümann,²⁷ C. Schwanda,^{9, 12} A. J. Schwartz,⁵ T. Seki,⁴⁸ S. Semenov,¹³ K. Senyo,²³ Y. Settai,⁴ R. Seuster,⁸ M. E. Sevior,²² T. Shibata,³⁰ H. Shibuya,⁴³ M. Shimoyama,²⁴

B. Shwartz,² V. Sidorov,² V. Siegle,³⁶ J. B. Singh,³³ N. Soni,³³ S. Stanič,^{51,‡} M. Starič,¹⁴
A. Sugi,²³ A. Sugiyama,³⁷ K. Sumisawa,⁹ T. Sumiyoshi,⁴⁸ K. Suzuki,⁹ S. Suzuki,⁵⁴
S. Y. Suzuki,⁹ S. K. Swain,⁸ K. Takahashi,⁴⁷ F. Takasaki,⁹ B. Takeshita,³² K. Tamai,⁹
Y. Tamai,³² N. Tamura,³⁰ K. Tanabe,⁴⁶ J. Tanaka,⁴⁶ M. Tanaka,⁹ G. N. Taylor,²²
A. Tchouvikov,³⁵ Y. Teramoto,³¹ S. Tokuda,²³ M. Tomoto,⁹ T. Tomura,⁴⁶ S. N. Tovey,²²
K. Trabelsi,⁸ T. Tsuboyama,⁹ T. Tsukamoto,⁹ K. Uchida,⁸ S. Uehara,⁹ K. Ueno,²⁷
T. Uglov,¹³ Y. Unno,³ S. Uno,⁹ N. Uozaki,⁴⁶ Y. Ushiroda,⁹ S. E. Vahsen,³⁵ G. Varner,⁸
K. E. Varvell,⁴¹ C. C. Wang,²⁷ C. H. Wang,²⁶ J. G. Wang,⁵³ M.-Z. Wang,²⁷
M. Watanabe,³⁰ Y. Watanabe,⁴⁷ L. Widhalm,¹² E. Won,¹⁶ B. D. Yabsley,⁵³ Y. Yamada,⁹
A. Yamaguchi,⁴⁵ H. Yamamoto,⁴⁵ T. Yamanaka,³² Y. Yamashita,²⁹ Y. Yamashita,⁴⁶
M. Yamauchi,⁹ H. Yanai,³⁰ Heyoung Yang,³⁹ J. Yashima,⁹ P. Yeh,²⁷ M. Yokoyama,⁴⁶
K. Yoshida,²³ Y. Yuan,¹¹ Y. Yusa,⁴⁵ H. Yuta,¹ C. C. Zhang,¹¹ J. Zhang,⁵¹ Z. P. Zhang,³⁸
Y. Zheng,⁸ V. Zhilich,² Z. M. Zhu,³⁴ T. Ziegler,³⁵ D. Žontar,^{20,14} and D. Zürcher,¹⁹

(The Belle Collaboration)

¹Aomori University, Aomori

²Budker Institute of Nuclear Physics, Novosibirsk

³Chiba University, Chiba

⁴Chuo University, Tokyo

⁵University of Cincinnati, Cincinnati, Ohio 45221

⁶University of Frankfurt, Frankfurt

⁷Gyeongsang National University, Chinju

⁸University of Hawaii, Honolulu, Hawaii 96822

⁹High Energy Accelerator Research Organization (KEK), Tsukuba

¹⁰Hiroshima Institute of Technology, Hiroshima

¹¹Institute of High Energy Physics,

Chinese Academy of Sciences, Beijing

¹²Institute of High Energy Physics, Vienna

¹³Institute for Theoretical and Experimental Physics, Moscow

¹⁴J. Stefan Institute, Ljubljana

¹⁵Kanagawa University, Yokohama

¹⁶Korea University, Seoul

¹⁷Kyoto University, Kyoto

¹⁸Kyungpook National University, Taegu

¹⁹Institut de Physique des Hautes Énergies, Université de Lausanne, Lausanne

²⁰University of Ljubljana, Ljubljana

²¹University of Maribor, Maribor

²²University of Melbourne, Victoria

²³Nagoya University, Nagoya

²⁴Nara Women's University, Nara

²⁵National Kaohsiung Normal University, Kaohsiung

²⁶National Lien-Ho Institute of Technology, Miao Li

²⁷Department of Physics, National Taiwan University, Taipei

²⁸H. Niewodniczanski Institute of Nuclear Physics, Krakow

²⁹Nihon Dental College, Niigata

³⁰Niigata University, Niigata

³¹*Osaka City University, Osaka*
³²*Osaka University, Osaka*
³³*Panjab University, Chandigarh*
³⁴*Peking University, Beijing*
³⁵*Princeton University, Princeton, New Jersey 08545*
³⁶*RIKEN BNL Research Center, Upton, New York 11973*
³⁷*Saga University, Saga*
³⁸*University of Science and Technology of China, Hefei*
³⁹*Seoul National University, Seoul*
⁴⁰*Sungkyunkwan University, Suwon*
⁴¹*University of Sydney, Sydney NSW*
⁴²*Tata Institute of Fundamental Research, Bombay*
⁴³*Toho University, Funabashi*
⁴⁴*Tohoku Gakuin University, Tagajo*
⁴⁵*Tohoku University, Sendai*
⁴⁶*Department of Physics, University of Tokyo, Tokyo*
⁴⁷*Tokyo Institute of Technology, Tokyo*
⁴⁸*Tokyo Metropolitan University, Tokyo*
⁴⁹*Tokyo University of Agriculture and Technology, Tokyo*
⁵⁰*Toyama National College of Maritime Technology, Toyama*
⁵¹*University of Tsukuba, Tsukuba*
⁵²*Utkal University, Bhubaneswar*
⁵³*Virginia Polytechnic Institute and State University, Blacksburg, Virginia 24061*
⁵⁴*Yokkaichi University, Yokkaichi*
⁵⁵*Yonsei University, Seoul*

(Dated: February 7, 2008)

Abstract

We present a precise measurement of the standard model CP -violation parameter $\sin 2\phi_1$ based on a sample of 152×10^6 $B\bar{B}$ pairs collected at the $\Upsilon(4S)$ resonance with the Belle detector at the KEKB asymmetric-energy e^+e^- collider. One neutral B meson is reconstructed in a $J/\psi K_S^0$, $\psi(2S)K_S^0$, $\chi_{c1}K_S^0$, $\eta_c K_S^0$, $J/\psi K^{*0}$, or $J/\psi K_L^0$ CP -eigenstate decay channel and the flavor of the accompanying B meson is identified from its decay products. From the asymmetry in the distribution of the time interval between the two B meson decay points, we obtain $\sin 2\phi_1 = 0.733 \pm 0.057(\text{stat}) \pm 0.028(\text{syst})$.

PACS numbers: 11.30.Er, 12.15.Hh, 13.25.Hw

In the standard model (SM), CP violation arises from an irreducible phase in the weak interaction quark-mixing matrix [Cabibbo-Kobayashi-Maskawa (CKM) matrix] [1]. In particular, the SM predicts a CP -violating asymmetry in the time-dependent rates for B^0 and \overline{B}^0 decays to a common CP eigenstate f_{CP} , where the transition is dominated by the $b \rightarrow c\bar{s}$ process, with negligible corrections from strong interactions [2]:

$$A(t) \equiv \frac{\Gamma(\overline{B}^0 \rightarrow f_{CP}) - \Gamma(B^0 \rightarrow f_{CP})}{\Gamma(\overline{B}^0 \rightarrow f_{CP}) + \Gamma(B^0 \rightarrow f_{CP})} = -\xi_f \sin 2\phi_1 \sin(\Delta m_d t), \quad (1)$$

where $\Gamma(B^0, \overline{B}^0 \rightarrow f_{CP})$ is the rate for B^0 or \overline{B}^0 to f_{CP} at a proper time t after production, ξ_f is the CP eigenvalue of f_{CP} , Δm_d is the mass difference between the two B^0 mass eigenstates, and ϕ_1 is one of the three interior angles of the CKM unitarity triangle, defined as $\phi_1 \equiv \pi - \arg(V_{tb}^* V_{td}/V_{cb}^* V_{cd})$. Non-zero values for $\sin 2\phi_1$ have been reported by the Belle and BaBar collaborations [3, 4, 5].

Belle's latest published measurement of $\sin 2\phi_1$ is based on a 78 fb^{-1} data sample (data set I) containing $85 \times 10^6 B\overline{B}$ pairs produced at the $\Upsilon(4S)$ resonance. In this paper, we report an improved measurement incorporating an additional 62 fb^{-1} (data set II) for a total of 140 fb^{-1} ($152 \times 10^6 B\overline{B}$ pairs). Changes exist in the analysis with respect to our earlier result [4]. We apply a new proper-time interval resolution function that reduces systematic uncertainties in $\sin 2\phi_1$ and also in Δm_d and lifetime (τ_{B^0}, τ_{B^+}) measurements. We introduce b -flavor-dependent wrong-tag fractions to accommodate possible differences between B^0 and \overline{B}^0 decays. We also adopt a multi-parameter fit to the flavor-specific control samples to obtain the resolution parameters and wrong-tag fractions simultaneously. There are other improvements in the estimation of background components, which become possible with increased statistics.

The data were collected with the Belle detector [6] at the KEKB asymmetric collider [7], which collides $8.0 \text{ GeV } e^-$ on $3.5 \text{ GeV } e^+$ at a small ($\pm 11 \text{ mrad}$) crossing angle. We use events where one of the B mesons decays to f_{CP} at time t_{CP} , and the other decays to a self-tagging state f_{tag} , which distinguishes B^0 from \overline{B}^0 , at time t_{tag} . The CP violation manifests itself as an asymmetry $A(\Delta t)$, where Δt is the proper time interval between the two decays: $\Delta t \equiv t_{CP} - t_{tag}$. At KEKB, the $\Upsilon(4S)$ resonance is produced with a boost of $\beta\gamma = 0.425$ nearly along the z axis defined as anti-parallel to the positron beam direction, and Δt can be determined as $\Delta t \simeq \Delta z/(\beta\gamma)c$, where Δz is the z distance between the f_{CP} and f_{tag} decay vertices, $\Delta z \equiv z_{CP} - z_{tag}$. The average value of Δz is approximately $200 \mu\text{m}$.

The Belle detector [6] is a large-solid-angle spectrometer that includes a silicon vertex detector (SVD), a central drift chamber (CDC), an array of aerogel threshold Čerenkov counters (ACC), time-of-flight (TOF) scintillation counters, and an electromagnetic calorimeter comprised of CsI(Tl) crystals (ECL) located inside a superconducting solenoid coil that provides a 1.5 T magnetic field. An iron flux-return located outside of the coil is instrumented to detect K_L^0 mesons and to identify muons (KLM).

We reconstruct B^0 decays to the following CP eigenstates [8]: $J/\psi K_S^0, \psi(2S)K_S^0, \chi_{c1}K_S^0, \eta_c K_S^0$ for $\xi_f = -1$ and $J/\psi K_L^0$ for $\xi_f = +1$. We also use $B^0 \rightarrow J/\psi K^{*0}$ decays where $K^{*0} \rightarrow K_S^0 \pi^0$. Here the final state is a mixture of even and odd CP , depending on the relative orbital angular momentum of the J/ψ and K^{*0} . We find that the final state is primarily $\xi_f = +1$; the $\xi_f = -1$ fraction is $0.19 \pm 0.02(\text{stat}) \pm 0.03(\text{syst})$ [9].

The reconstruction and selection criteria for all f_{CP} channels used in the measurement are described in detail elsewhere [3]. J/ψ and $\psi(2S)$ mesons are reconstructed via their

decays to $\ell^+\ell^-$ ($\ell = \mu, e$). The $\psi(2S)$ is also reconstructed via $J/\psi\pi^+\pi^-$, and the χ_{c1} via $J/\psi\gamma$. The η_c is detected in the $K_S^0K^-\pi^+$, $K^+K^-\pi^0$, and $p\bar{p}$ modes. For the $J/\psi K_S^0$ mode, we use $K_S^0 \rightarrow \pi^+\pi^-$ and $\pi^0\pi^0$ decays; for other modes we only use $K_S^0 \rightarrow \pi^+\pi^-$. For reconstructed $B \rightarrow f_{CP}$ candidates other than $J/\psi K_L^0$, we identify B decays using the energy difference $\Delta E \equiv E_B^{\text{cms}} - E_{\text{beam}}^{\text{cms}}$ and the beam-energy constrained mass $M_{\text{bc}} \equiv \sqrt{(E_{\text{beam}}^{\text{cms}})^2 - (p_B^{\text{cms}})^2}$, where $E_{\text{beam}}^{\text{cms}}$ is the beam energy in the center-of-mass system (cms) of the $\Upsilon(4S)$ resonance, and E_B^{cms} and p_B^{cms} are the cms energy and momentum of the reconstructed B candidate, respectively.

Candidate $B^0 \rightarrow J/\psi K_L^0$ decays are selected by requiring ECL and/or KLM hit patterns that are consistent with the presence of a shower induced by a K_L^0 meson. The centroid of the shower is required to be within a 45° cone centered on the K_L^0 direction inferred from two-body decay kinematics and the measured four-momentum of the J/ψ .

We perform a multi-parameter fit to flavor-specific control samples to obtain wrong-tag fractions and parameters for the resolution function simultaneously. We select $B^0 \rightarrow D^{*-}\ell^+\nu$, $J/\psi K^{*0}(K^+\pi^-)$, $D^{*-}\pi^+$, $D^-\pi^+$, $D^{*-}\rho^+$, and $J/\psi K_S^0(\ell^+\ell^-)$ (for resolution parameters only) for B^0 decays, and $B^+ \rightarrow \overline{D}^0\pi^+$ and $J/\psi K^+$ for B^+ decays. The total numbers of candidates (N_{ev}) and purities (p) are $N_{\text{ev}} = 124118$ and $p = 0.82$ for B^0 decays, and $N_{\text{ev}} = 57305$ and $p = 0.81$ for B^+ decays. The fit uses free parameters for wrong-tag fractions (12), for the resolution function (14), for the B^+ background in B^0 decays (3), Δm_d , τ_{B^0} and τ_{B^+} . The total number of parameters in the fit is 32. We add two parameters to the resolution function described in [10] to obtain an improved description of the effect of charmed particle decays in the f_{tag} vertex. We test the new fit method and parameterization with a large number of Monte Carlo (MC) events. A fit to the MC control sample yields $\Delta m_d = (0.488 \pm 0.002)$ ps $^{-1}$, $\tau_{B^0} = (1.539 \pm 0.003)$ ps and $\tau_{B^+} = (1.679 \pm 0.004)$ ps for the input values of $\Delta m_d = 0.489$ ps $^{-1}$, $\tau_{B^0} = 1.541$ ps and $\tau_{B^+} = 1.674$ ps, respectively. The obtained wrong-tag fractions are also found to be correct. The unbinned maximum-likelihood fit to data yields $\Delta m_d = [0.511 \pm 0.005(\text{stat})]$ ps $^{-1}$, $\tau_{B^0} = [1.533 \pm 0.008(\text{stat})]$ ps and $\tau_{B^+} = [1.634 \pm 0.011(\text{stat})]$ ps, where the errors are statistical only. The results are consistent with the present world average values [11].

Charged leptons, pions, kaons, and Λ baryons that are not associated with a reconstructed CP eigenstate decay are used to identify the b -flavor of the accompanying B meson. The tagging algorithm is identical to the one used in reference [4]. We use two parameters, q and r , to represent the tagging information. The first, q , has the discrete value $+1$ (-1) when the tag-side B meson is likely to be a B^0 (\overline{B}^0), and the parameter r is an event-by-event Monte Carlo-determined flavor-tagging dilution parameter that ranges from $r = 0$ for no flavor discrimination to $r = 1$ for an unambiguous flavor assignment. It is used only to sort data into six intervals of r , according to estimated flavor purity. We determine directly from data the average wrong-tag probabilities, $w_l \equiv (w_l^+ + w_l^-)/2$ ($l = 1, 6$), and differences between B^0 and \overline{B}^0 decays, $\Delta w_l \equiv w_l^+ - w_l^-$, where $w_l^{+(-)}$ is the wrong-tag probability for the $B^0(\overline{B}^0)$ decay in each r interval. The event fractions and wrong-tag fractions are summarized in Table I. The total effective tagging efficiency is determined to be $\epsilon_{\text{eff}} \equiv \sum_{l=1}^6 \epsilon_l (1 - 2w_l)^2 = 0.287 \pm 0.005$, where ϵ_l is the event fraction for each r interval. The error includes both statistical and systematic uncertainties.

The vertex position for the f_{CP} decay is reconstructed using leptons from J/ψ decays or charged hadrons from η_c decays, and that for f_{tag} is obtained with well reconstructed tracks that are not assigned to f_{CP} . Tracks that are consistent with coming from a $K_S^0 \rightarrow \pi^+\pi^-$

TABLE I: The event fractions ϵ_l , wrong-tag fractions w_l , wrong-tag fraction differences Δw_l , and average effective tagging efficiencies $\epsilon_{\text{eff}}^l = \epsilon_l(1 - 2w_l)^2$ for each r interval. The errors include both statistical and systematic uncertainties. The event fractions are obtained from the $J/\psi K_S^0$ simulation.

| l | r interval | ϵ_l | w_l | Δw_l | ϵ_{eff}^l |
|-----|---------------|--------------|-------------------|--------------------|---------------------------|
| 1 | 0.000 – 0.250 | 0.398 | 0.464 ± 0.006 | -0.011 ± 0.006 | 0.002 ± 0.001 |
| 2 | 0.250 – 0.500 | 0.146 | 0.331 ± 0.008 | $+0.004 \pm 0.010$ | 0.017 ± 0.002 |
| 3 | 0.500 – 0.625 | 0.104 | 0.231 ± 0.009 | -0.011 ± 0.010 | 0.030 ± 0.002 |
| 4 | 0.625 – 0.750 | 0.122 | 0.163 ± 0.008 | -0.007 ± 0.009 | 0.055 ± 0.003 |
| 5 | 0.750 – 0.875 | 0.094 | 0.109 ± 0.007 | $+0.016 \pm 0.009$ | 0.057 ± 0.002 |
| 6 | 0.875 – 1.000 | 0.136 | 0.020 ± 0.005 | $+0.003 \pm 0.006$ | 0.126 ± 0.003 |

decay are not used. Each vertex position is required to be consistent with the interaction region profile, determined run-by-run, smeared in the r - ϕ plane to account for the B meson decay length. With these requirements, we are able to determine a vertex even with a single track; the fraction of single-track vertices is about 10% for z_{CP} and 22% for z_{tag} . The proper-time interval resolution function $R_{\text{sig}}(\Delta t)$ is formed by convolving four components: the detector resolutions for z_{CP} and z_{tag} , the shift in the z_{tag} vertex position due to secondary tracks originating from charmed particle decays, and the kinematic approximation that the B mesons are at rest in the cms [10]. A small component of broad outliers in the Δz distribution, caused by mis-reconstruction, is represented by a Gaussian function. We determine fourteen resolution parameters from the aforementioned fit to the control samples. We find that the average Δt resolution is ~ 1.43 ps (rms). The width of the outlier component is determined to be (39 ± 2) ps; the fractions of the outlier components are $(2.1 \pm 0.6) \times 10^{-4}$ for events with both vertices reconstructed with more than one track, and $(3.1 \pm 0.1) \times 10^{-2}$ for events with at least one single-track vertex.

After flavor tagging and vertexing, we find 5417 events in total in the signal region, which are used for the $\sin 2\phi_1$ determination. Table II lists the numbers of candidates, N_{ev} , and the estimated signal purity for each f_{CP} mode. Figure 1 shows the M_{bc} distribution after applying mode-dependent requirements on ΔE for all B^0 candidates except for $B^0 \rightarrow J/\psi K_L^0$. There are 3085 entries in total in the signal region defined as $5.27 < M_{bc} < 5.29$ GeV/c^2 . Figure 2 shows the p_B^{cms} distribution for $B^0 \rightarrow J/\psi K_L^0$ candidates. We find 2332 entries in the $0.20 \leq p_B^{\text{cms}} \leq 0.45$ GeV/c signal region.

Figure 3 shows the observed Δt distributions for the $q\xi_f = +1$ and $q\xi_f = -1$ event samples (top), the asymmetry between two samples with $0 < r \leq 0.5$ (middle) and with $0.5 < r \leq 1.0$ (bottom). The asymmetry in the region $0.5 < r \leq 1.0$, where wrong-tag fractions are small as shown in Table I, clearly demonstrates large CP violation.

We determine $\sin 2\phi_1$ from an unbinned maximum-likelihood fit to the observed Δt distributions. The probability density function (PDF) expected for the signal distribution is given by

$$\mathcal{P}_{\text{sig}}(\Delta t, q, w_l, \Delta w_l, \xi_f) = \frac{e^{-|\Delta t|/\tau_{B^0}}}{4\tau_{B^0}} [1 - q\Delta w_l - q\xi_f(1 - 2w_l)\sin 2\phi_1 \sin(\Delta m_d \Delta t)], \quad (2)$$

where we fix the B^0 lifetime τ_{B^0} and mass difference Δm_d at their world average values [11]. Each PDF is convolved with the appropriate $R_{\text{sig}}(\Delta t)$ to determine the likelihood value for

TABLE II: The numbers of reconstructed $B \rightarrow f_{CP}$ candidates after flavor tagging and vertex reconstruction, N_{ev} , and the estimated signal purity, p , in the signal region for each f_{CP} mode. J/ψ mesons are reconstructed in $J/\psi \rightarrow \mu^+ \mu^-$ or $e^+ e^-$ decays. Candidate K_S^0 mesons are reconstructed in $K_S^0 \rightarrow \pi^+ \pi^-$ decays unless otherwise written explicitly.

| Mode | ξ_f | N_{ev} | p |
|-------------------------------------|---------|-----------------|-------------------|
| $J/\psi K_S^0$ | -1 | 1997 | 0.976 ± 0.001 |
| $J/\psi K_S^0(\pi^0 \pi^0)$ | -1 | 288 | 0.82 ± 0.02 |
| $\psi(2S)(\ell^+ \ell^-)K_S^0$ | -1 | 145 | 0.93 ± 0.01 |
| $\psi(2S)(J/\psi \pi^+ \pi^-)K_S^0$ | -1 | 163 | 0.88 ± 0.01 |
| $\chi_{c1}(J/\psi \gamma)K_S^0$ | -1 | 101 | 0.92 ± 0.01 |
| $\eta_c(K_S^0 K^- \pi^+)K_S^0$ | -1 | 123 | 0.72 ± 0.03 |
| $\eta_c(K^+ K^- \pi^0)K_S^0$ | -1 | 74 | 0.70 ± 0.04 |
| $\eta_c(p\bar{p})K_S^0$ | -1 | 20 | 0.91 ± 0.02 |
| All with $\xi_f = -1$ | -1 | 2911 | 0.933 ± 0.002 |
| $J/\psi K^{*0}(K_S^0 \pi^0)$ | +1(81%) | 174 | 0.93 ± 0.01 |
| $J/\psi K_L^0$ | +1 | 2332 | 0.60 ± 0.03 |

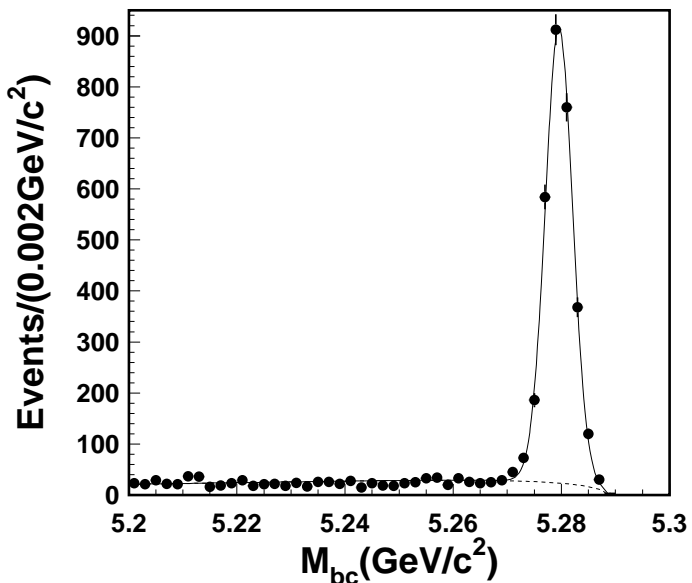


FIG. 1: The beam-energy constrained mass distribution within the ΔE signal region for all f_{CP} modes other than $J/\psi K_L^0$. The solid curve shows the fit to signal plus background distributions, and the dashed curve shows the background contribution.

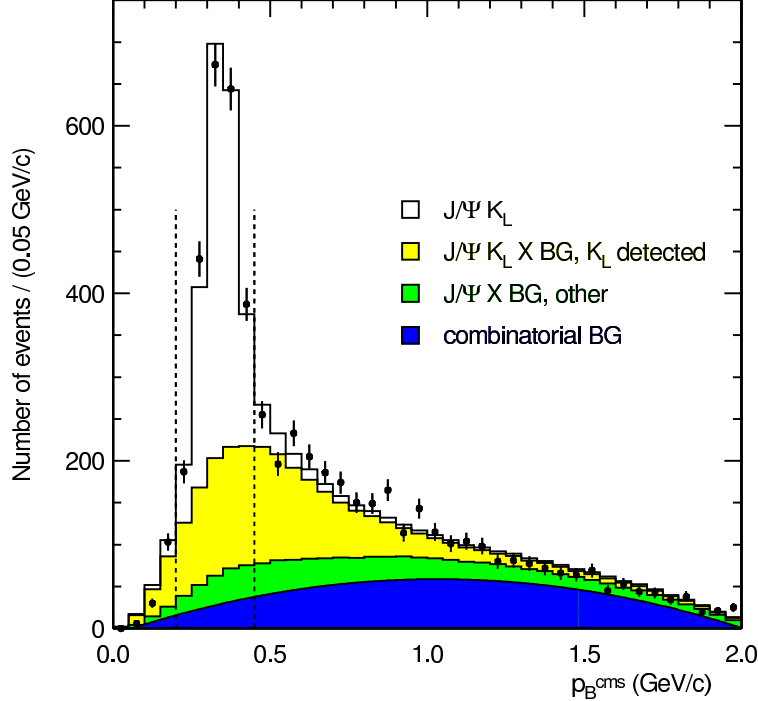


FIG. 2: The p_B^{cms} distribution for $B^0 \rightarrow J/\psi K_L^0$ candidates with the results of the fit. The dashed lines indicate the signal region ($0.20 \leq p_B^{\text{cms}} \leq 0.45$ GeV/ c).

each event as a function of $\sin 2\phi_1$:

$$P_i = (1 - f_{\text{ol}}) \int [f_{\text{sig}} \mathcal{P}_{\text{sig}}(\Delta t', q, w_l, \Delta w_l, \xi_f) R_{\text{sig}}(\Delta t - \Delta t') + (1 - f_{\text{sig}}) \mathcal{P}_{\text{bkg}}(\Delta t') R_{\text{bkg}}(\Delta t - \Delta t')] d\Delta t' + f_{\text{ol}} P_{\text{ol}}(\Delta t), \quad (3)$$

where f_{sig} is the signal fraction calculated as a function of p_B^{cms} for $J/\psi K_L^0$ and of ΔE and M_{bc} for other modes. $\mathcal{P}_{\text{bkg}}(\Delta t)$ is the PDF for combinatorial background events, which is modeled as a sum of exponential and prompt components. It is convolved with a sum of two Gaussians, R_{bkg} , which is regarded as a resolution function for the background. To account for a small number of events that give large Δt in both the signal and background, we introduce the PDF of the outlier component, P_{ol} , and its fraction f_{ol} . The only free parameter in the final fit is $\sin 2\phi_1$, which is determined by maximizing the likelihood function $L = \prod_i P_i$, where the product is over all events. The result of the fit is

$$\sin 2\phi_1 = 0.733 \pm 0.057(\text{stat}) \pm 0.028(\text{syst}).$$

Sources of systematic error include uncertainties in the flavor tagging (0.014), in the vertex reconstruction (0.013), in the background fractions for $B^0 \rightarrow J/\psi K_L^0$ (0.012) and for other modes (0.007), in the resolution function (0.008), a possible bias in the $\sin 2\phi_1$ fit (0.008), and an effect of interferences [12] in the f_{tag} final state (0.008). The errors introduced by uncertainties in Δm_d , τ_{B^0} and in the background Δt distribution, are less than 0.005.

Several checks on the measurement are performed. Table III lists the results obtained by applying the same analysis to various subsamples. All values are statistically consistent with

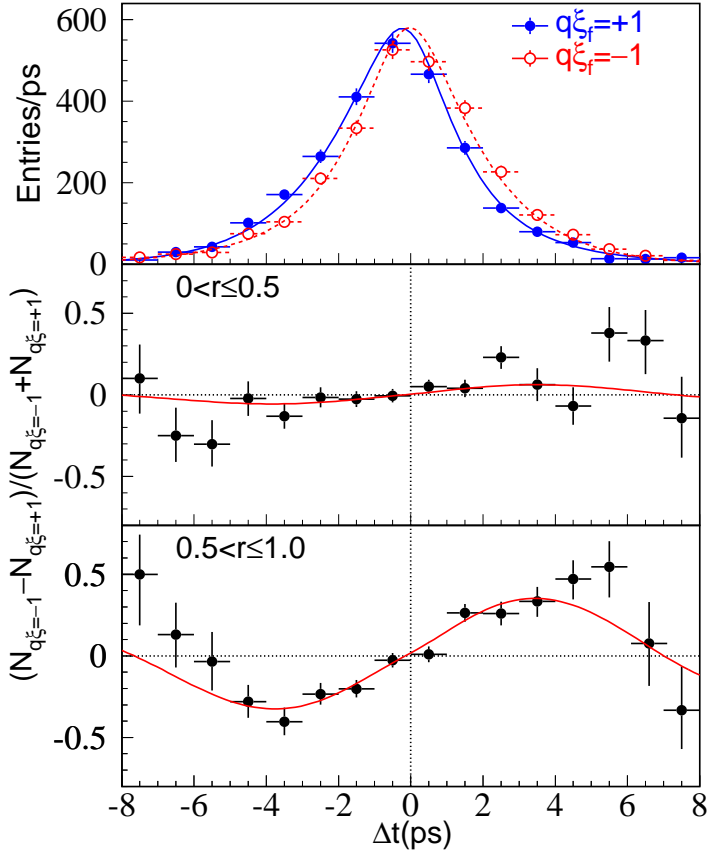


FIG. 3: The Δt distributions for the events with $q\xi_f = -1$ (open points) and $q\xi_f = +1$ (solid points) with all modes combined (top), the asymmetry in each Δt bin between $q\xi_f = -1$ and $q\xi_f = +1$ samples with $0 < r \leq 0.5$ (middle), and with $0.5 < r \leq 1$ (bottom). The results of the global unbinned maximum-likelihood fit ($\sin 2\phi_1 = 0.733$) are also shown.

each other. Figure 4 shows the raw asymmetries and the fit results for $(c\bar{c})K_S^0$ (top) and $J/\psi K_L^0$ (bottom). A fit to the non- CP eigenstate modes $B^0 \rightarrow D^{*-} \ell^+ \nu$ and $J/\psi K^{*0}(K^+ \pi^-)$, where no asymmetry is expected, yields $0.012 \pm 0.013(\text{stat})$.

The signal PDF for a neutral B meson decaying into a CP eigenstate [Eq. (2)] can be expressed in a more general form as

$$\begin{aligned} \mathcal{P}_{\text{sig}}(\Delta t, q, w_l, \Delta w_l) \\ = \frac{e^{-|\Delta t|/\tau_{B^0}}}{4\tau_{B^0}} \left\{ 1 - q\Delta w_l + q(1 - 2w_l) [\mathcal{S} \sin(\Delta m_d \Delta t) + \mathcal{A} \cos(\Delta m_d \Delta t)] \right\}, \end{aligned} \quad (4)$$

where $\mathcal{S} \equiv 2\mathcal{I}m(\lambda)/(|\lambda|^2 + 1)$, $\mathcal{A} \equiv (|\lambda|^2 - 1)/(|\lambda|^2 + 1)$, and λ is a complex parameter that depends on both B^0 - \overline{B}^0 mixing and on the amplitudes for B^0 and \overline{B}^0 decay to a CP

TABLE III: The numbers of candidate events, N_{ev} , and values of $\sin 2\phi_1$ for various subsamples (statistical errors only).

| Sample | N_{ev} | $\sin 2\phi_1$ |
|---|-----------------|-------------------|
| $J/\psi K_S^0(\pi^+\pi^-)$ | 1997 | 0.67 ± 0.08 |
| $J/\psi K_S^0(\pi^0\pi^0)$ | 288 | 0.72 ± 0.20 |
| $\psi(2S)K_S^0$ | 308 | 0.89 ± 0.20 |
| $\chi_{c1}K_S^0$ | 101 | 1.54 ± 0.49 |
| $\eta_c K_S^0$ | 217 | 1.32 ± 0.29 |
| All with $\xi_f = -1$ | 2911 | 0.73 ± 0.06 |
| $J/\psi K_L^0$ | 2332 | 0.80 ± 0.13 |
| $J/\psi K^{*0}(K_S^0\pi^0)$ | 174 | 0.10 ± 0.45 |
| $f_{\text{tag}} = B^0$ ($q = +1$) | 2717 | 0.72 ± 0.09 |
| $f_{\text{tag}} = \bar{B}^0$ ($q = -1$) | 2700 | 0.74 ± 0.08 |
| $0 < r \leq 0.5$ | 2985 | 0.95 ± 0.26 |
| $0.5 < r \leq 0.75$ | 1224 | 0.68 ± 0.11 |
| $0.75 < r \leq 1$ | 1208 | 0.74 ± 0.07 |
| data set I (78 fb^{-1}) | 3013 | 0.73 ± 0.07 |
| data set II (62 fb^{-1}) | 2404 | 0.74 ± 0.09 |
| All | 5417 | 0.733 ± 0.057 |

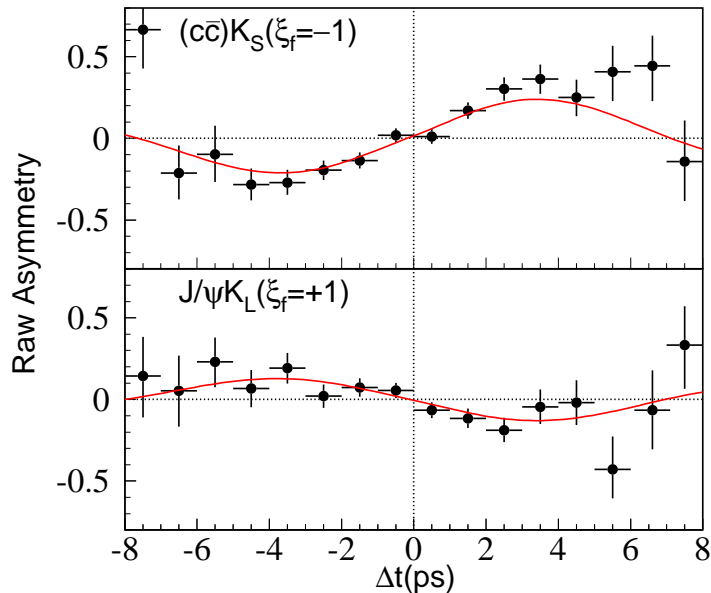


FIG. 4: The raw asymmetries for $(cc)K_S^0$ ($\xi_f = -1$) (top) and $J/\psi K_L^0$ ($\xi_f = +1$) (bottom). The curves are the results of the global unbinned maximum-likelihood fit.

eigenstate. The presence of the cosine term ($|\lambda| \neq 1$) would indicate direct CP violation; the value for $\sin 2\phi_1$ reported above is determined with the assumption $|\lambda| = 1$, as $|\lambda|$ is expected to be very close to one in the SM. In order to test this assumption, we also performed a fit using the expression above with $a_{CP} \equiv -\xi_f \text{Im}\lambda/|\lambda|$ and $|\lambda|$ as free parameters, keeping everything else the same. We obtain

$$|\lambda| = 1.007 \pm 0.041(\text{stat}), \\ a_{CP} = 0.733 \pm 0.057(\text{stat}),$$

for all CP modes combined. This result is consistent with the assumption used in our analysis.

We wish to thank the KEKB accelerator group for the excellent operation of the KEKB accelerator. We acknowledge support from the Ministry of Education, Culture, Sports, Science, and Technology of Japan and the Japan Society for the Promotion of Science; the Australian Research Council and the Australian Department of Education, Science and Training; the National Science Foundation of China under contract No. 10175071; the Department of Science and Technology of India; the BK21 program of the Ministry of Education of Korea and the CHEP SRC program of the Korea Science and Engineering Foundation; the Polish State Committee for Scientific Research under contract No. 2P03B 01324; the Ministry of Science and Technology of the Russian Federation; the Ministry of Education, Science and Sport of the Republic of Slovenia; the National Science Council and the Ministry of Education of Taiwan; and the U.S. Department of Energy.

* on leave from Fermi National Accelerator Laboratory, Batavia, Illinois 60510

† on leave from University of Pittsburgh, Pittsburgh PA 15260

‡ on leave from Nova Gorica Polytechnic, Nova Gorica

- [1] M. Kobayashi and T. Maskawa, Prog. Theor. Phys. **49**, 652 (1973).
- [2] A. B. Carter and A. I. Sanda, Phys. Rev. D **23**, 1567 (1981); I. I. Bigi and A. I. Sanda, Nucl. Phys. **B193**, 85 (1981).
- [3] Belle Collaboration, K. Abe *et al.*, Phys. Rev. Lett. **87**, 091802 (2001); Phys. Rev. D **66**, 032007 (2002).
- [4] Belle Collaboration, K. Abe *et al.*, Phys. Rev. D **66**, 071102 (2002).
- [5] BaBar Collaboration, B. Aubert *et al.*, Phys. Rev. Lett. **87**, 091801 (2001); Phys. Rev. D **66**, 032003 (2002); Phys. Rev. Lett. **89**, 201802 (2002).
- [6] Belle Collaboration, A. Abashian *et al.*, Nucl. Instrum. Methods Phys. Res. A **479**, 117 (2002).
- [7] S. Kurokawa and E. Kikutani *et al.*, Nucl. Instrum. Methods A **499**, 1 (2003).
- [8] Throughout this paper, when a decay mode is quoted, the inclusion of the charge conjugate mode is implied.
- [9] Belle Collaboration, K. Abe *et al.*, Phys. Lett. B **538**, 11 (2002).
- [10] H. Tajima *et al.*, hep-ex/0301026.
- [11] Particle Data Group, K. Hagiwara *et al.*, Particle Listings in the 2003 Review of Particle Physics, http://www-pdg.lbl.gov/2003/contents_listings.html.
- [12] O. Long, M. Baak, R. N. Cahn and D. Kirkby, hep-ex/0303030.